Fall 2009

Height of the planetary boundary layer during ICEALOT 2008

Virginia Sawyer
University of New Hampshire, Durham

HEIGHT OF THE PLANETARY BOUNDARY LAYER DURING ICEALOT 2008

BY

VIRGINIA SAWYER
BS, Cornell University, 2007

THESIS

Submitted to the University of New Hampshire
in Partial Fulfillment of
the Requirements for the Degree of

Master of Science
in
Earth Science

September, 2009

This thesis has been examined and approved.

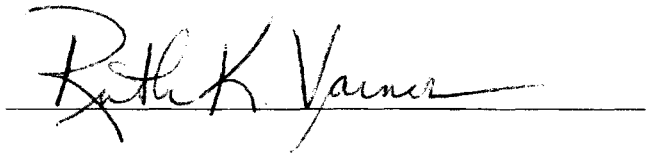

Thesis Director, Dr. Ruth K. Varner, Research Assistant Professor of EOS and Earth Sciences

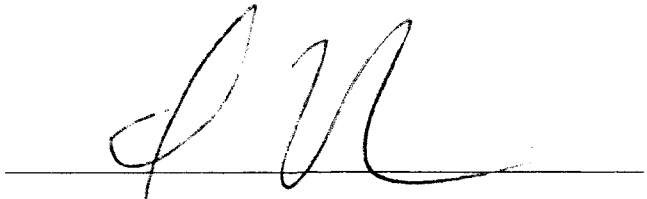

Dr. Douglas C. Vandemark, Research Associate Professor of EOS and Earth Sciences

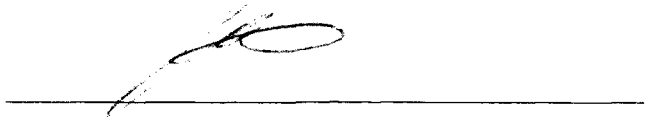

Dr. Ellsworth J. Welton, NASA Goddard Space Flight Center

August 6, 2009

Date

TABLE OF CONTENTS

LIST OF FIGURES

Page

Page

ABSTRACT

HEIGHT OF THE PLANETARY BOUNDARY LAYER DURING ICEALOT 2008

by

Virginia Sawyer

University of New Hampshire, September, 2009

The planetary boundary layer (PBL) is a buoyantly stable feature of the lower troposphere that restricts mixing between the surface air and the free troposphere aloft. In the Arctic, PBL behavior is particularly important to atmospheric chemistry because most anthropogenic pollutants enter the region via long-range transport rather than local emissions, and therefore must pass through the PBL. PBL heights can be detected in the backscatter signal of the MPLNET aerosol lidar that was part of the ICEALOT research campaign of March and April 2008, along with observations of elevated aerosol plumes and cloud formation. Features in the MPLNET backscatter are compared to sonde data from the cruise and to backscatter profiles from overpasses by the CALIPSO satellite.

INTRODUCTION

The planetary boundary layer (PBL) is the height at which the lower troposphere transitions from surface influences on temperature, moisture, and dynamics to approximately geostrophic flow aloft. Typically occurring below 1 km in the marine Arctic, it is defined by a temperature inversion that creates a layer of buoyant stability. Because the inversion inhibits mixing between the surface air and the free troposphere, aerosol pollutants that remain below the PBL height generally deposit within a few kilometers of their origin, while aerosols above the PBL are included in long-range transport (Seinfeld and Pandis 2006). Because there are few anthropogenic sources of aerosol at high latitudes, long-range transport of emissions from the midlatitudes makes up a large part of air pollution north of the Arctic Circle; the behavior of the planetary boundary layer thus becomes especially important during the annual peak in aerosol concentrations known as the Arctic haze.

Arctic haze events were first reported by pilots in the 1950s (Mitchell 1957). They typically occur over the Arctic Ocean rather than over the land surface, in patches several hundred kilometers across. In extreme cases, as in the spring of 2006 at Ny-Ålesund, Svalbard, the haze becomes thick enough to reduce surface visibility (Law and Stohl 2007) but more often it is invisible to ground observers. It peaks in March and April, shortly after the polar sunrise. During the winter, the polar front creates a dome-like barrier over the pole which prevents pollutants from entering the Arctic lower troposphere; when the region begins to

warm in spring, the front weakens and mixing between polar and midlatitude air becomes more prevalent. Aerosols accumulate through the spring at all levels of the troposphere until precipitation rates and photochemical processes accelerate in the summer, allowing the haze to dissipate (Quinn et al. 2007).

The chemical composition of Arctic haze is a mixture of sea salt, sulfates, and organic carbon, with smaller amounts of black carbon, ammonium, nitrates, and silicate dust. While much of the haze is of natural origin, anthropogenic pollutants within the haze include trace levels of mercury and other heavy metals (Heidam et al. 2004) which pose a contamination hazard for the people and ecosystems of the Arctic. In addition, the interference by deposited particulate matter, especially black carbon, with the strong ice-albedo feedback mechanism has a warming effect on the climate of the Arctic and the rest of the world (IPCC 2007). The possibility that melting sea ice will lead to increased shipping across the Arctic Ocean in future decades means that local sources of anthropogenic emissions are likely to increase, adding to the impact that particles from midlatitude sources already have on a vulnerable region.

The effect of the planetary boundary layer on atmospheric transport is especially important in the Arctic, where there are few local sources of anthropogenic emissions. Aerosols derived from biomass burning, transportation, and industrial processes in the midlatitudes are observed as components of the Arctic haze, having arrived in the region via long-range transport in the free troposphere. They enter the surface air of the Arctic from aloft, passing through the PBL. Later in spring, most aerosol is removed from the atmosphere by wet deposition, involving precipitation that forms below the PBL. The Arctic haze

depends on mixing through the planetary boundary layer for aerosol pollution to affect the surface, but also for much of the removal mechanism that restricts the pollution to springtime. Changes in the planetary boundary layer height over a time scale of hours make it more likely that mixing will occur; the behavior of the PBL height therefore determines the vertical structure of the Arctic haze and the ability of removal processes to deposit aerosol from the Arctic atmosphere.

Because the planetary boundary layer determines so much of the behavior of particles with height, it is possible to infer the PBL height from the structure of the particle backscatter profile measured by a ground-based, upward-directed aerosol lidar. According to the classical definition, the well-mixed air below the boundary has almost uniform concentrations of aerosol with height, and this mixed layer is polluted relative to the free troposphere above the PBL (Melfi et al. 1985). By contrast, the free troposphere is generally cleaner, and the aerosols that are present are stratified with height; this reflects the greater buoyant stability of the free troposphere and the barrier to aerosol transport above the PBL. Cloud data in the same backscatter profile sometimes makes the PBL height more obvious, because the temperature inversion that defines the planetary boundary layer sometimes forms due to latent heat release from condensation (Davis et al. 2000). In the Arctic, the surface receives too little insolation to cause much atmospheric convection. However, because of the difference between the sea surface temperature and the temperature of the air above it, fogs (Figure 1) and low clouds are common. These control the PBL height when they are present (Tjernström 2005). The Arctic also has lower concentrations of aerosol than most midlatitude study sites, so the backscatter

signal is weaker; but despite these differences, the assumptions used to characterize atmospheric structure in lidar backscatter profiles are applicable to the Arctic.

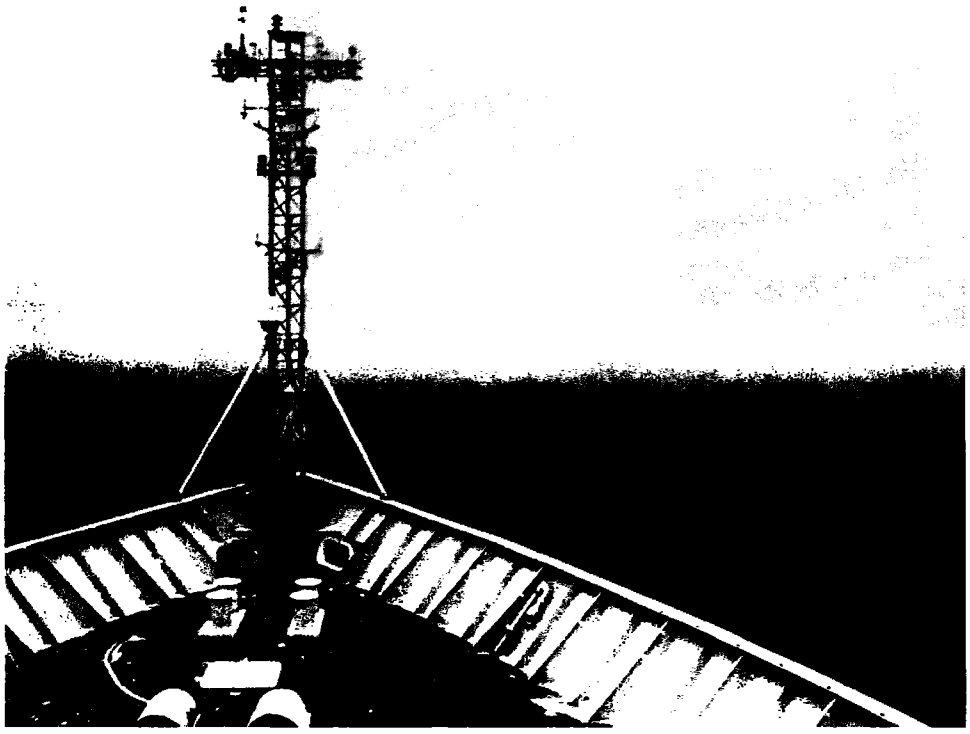

Figure 1. Steam fog as seen from the bow of the *R/V Knorr* on 15 April 2008.

The PBL height found this way represents only the center point of a transition zone between the mixed layer and the free troposphere. In some atmospheric conditions, the transition zone is the layer in which turbulent mixing and entrainment can occur from the free troposphere into the mixed layer. In other, more stable conditions, the transition zone simply represents the depth of the temperature inversion, which may be over a kilometer; the PBL itself is better described in these cases as a range of altitudes rather than a single height (Brooks 2003). While it is possible to expand the algorithm described in the methods section to find the depth of the transition zone, defining the PBL as its

midpoint, this is computationally too intensive to be suitable for large datasets with ongoing observations taking place.

Lidar-derived PBL heights have advantages in spatial and temporal resolution over more direct methods of PBL detection, such as using the temperature and humidity data from sonde launches or satellite observation. Sonde launches are too infrequent to detect short-term changes in the PBL as they develop, such as diurnal variation or the formation and movement of cloud layers. Palm et al. (1998) discussed the fact that satellite temperature and humidity data, while having the advantage of near-global spatial coverage, have a vertical resolution on the order of 1 km—too coarse to resolve the PBL, much less changes to its height in the low hundreds of meters. While aerosol lidar does not collect the data necessary to detect temperature inversions directly, the distribution of aerosols with height is a useful proxy for the PBL, available in continuous measurements at short time intervals. Space-based lidar such as the instrument aboard NASA's CALIPSO satellite can detect the PBL in the same way, with the excellent spatial coverage of any polar-orbiting satellite—and as of April 2009, CALIPSO has operated continuously for three years. Due to the opacity of many cloud types at aerosol lidar wavelengths and the greater distance from the PBL itself, however, CALIPSO is somewhat less reliable than ground-based lidar for this purpose.

The purpose of this thesis is to evaluate the use of aerosol lidar backscatter as a proxy for PBL height in the Arctic Ocean, where conditions are often very different from those in the land-based, midlatitude sites more typically observed with the instrument. Juxtaposed with meteorological and chemical

observations from the same cruise, the lidar also helps to provide insights into processes that define the role of the Arctic in global atmospheric chemistry and climate, especially events at altitudes that cannot be sampled directly. Aerosol lidar is a useful complement to other sources of atmospheric chemistry data.

CHAPTER I

EXPERIMENT AND INSTRUMENTATION

The International Chemistry Experiment in the Arctic Lower Troposphere (ICEALOT) was a campaign during the spring of 2008 that specifically targeted the Arctic haze for study. Between 19 March and 12 April, the *R/V Knorr* traveled from Woods Hole, Massachusetts to Tromsø, Norway. The second leg of the cruise proceeded in open water past the Svalbard coast to 80° N, before turning southward, passing the island of Jan Mayen, and ending in Reykjavík, Iceland on 24 April (Figure 2). The cruise was a NOAA contribution to POLARCAT for the International Polar Year, with a goal of understanding the composition, transport, and chemical evolution of aerosols and gases that make up the Arctic haze.

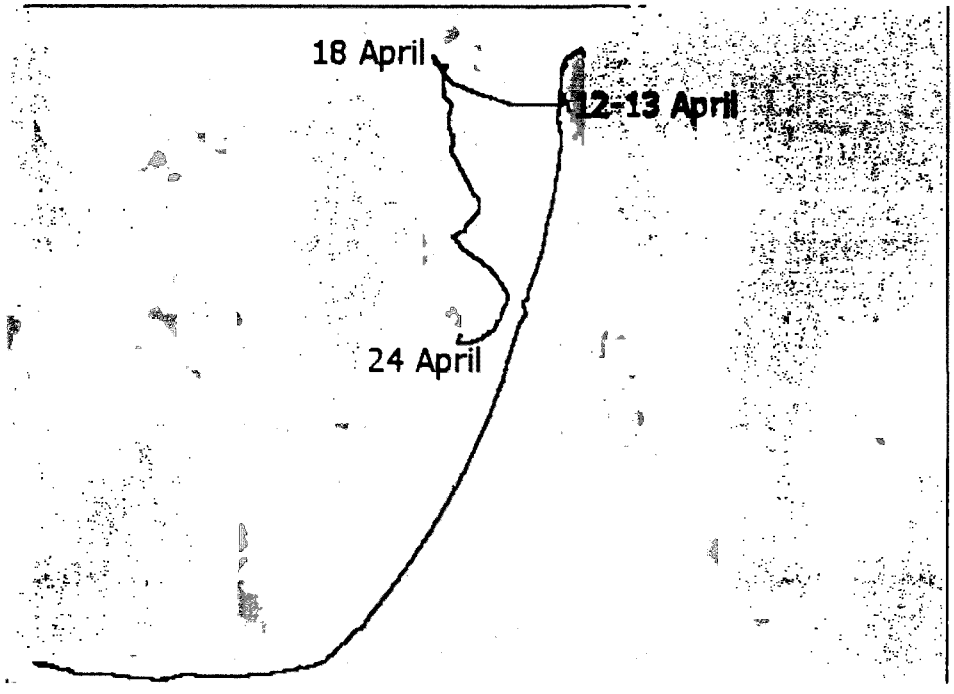

Figure 2. Path of the *R/V Knorr* during ICEALOT.

Among the instruments aboard ship was an aerosol lidar from NASA MPLNET. Light detection and ranging (lidar) has many applications in the earth and environmental sciences, among which is the detection of clouds and aerosols in the atmosphere (Morille et al. 2007). Cloud and aerosol lidar operates by aiming a laser beam of visible or near-IR light at a target column of atmosphere. Because clouds, aerosols and to a lesser extent the molecules of clean air all scatter light at these wavelengths, some of the energy from the laser returns to the instrument after it is deflected from particles in the atmosphere. A telescope and time-of-flight measurement allows the lidar to detect returning photons and sort them by the height of the particle that deflected them (Wandinger 2005). The resulting backscatter profile measures the energy deflected at different heights in the atmosphere, providing an estimate of relative aerosol concentration with height and the location of any clouds.

The lidar aboard ICEALOT used a 527-nm laser with a pulse energy on the order of microjoules, which was expanded through the shared transmitter/receiver telescope at a repetition rate of 2500 Hz (Campbell et al. 2002). These features of the instrument render it eye-safe, which made it possible to operate the lidar continuously for the length of the cruise. MPLNET lidars are designed to work for long periods with minimal human involvement, pointed vertically so that the backscatter profile is ground-upward—the reverse of lidar data taken from airborne or spaceborne instruments. The lidar was situated in an enclosure that was bolted to the deck of the ship and temperature-controlled to avoid distorting the telescope optics. A window in the enclosure allowed the laser to be beamed upward, and an Ethernet line to a nearby storage van

allowed access to its controls without exposing the lidar to the open air (Figure 3). Early in the cruise, it became necessary to shield the window lens from sideways spray, and salt and moisture were regularly cleaned from it throughout the experiment. Lidar dark count and afterpulse measurements were taken weekly for calibration purposes. The height bins for backscattered photons were set to 75-m vertical resolution, and backscatter profiles were taken once per minute.

Additional aerosol lidar data was available from the CALIPSO satellite, which crossed overhead on four occasions during the cruise. CALIPSO's primary instrument is CALIOP, a downward-facing aerosol lidar with a 532-nm laser. As part of the NASA A-train satellite constellation, CALIPSO provides lidar-derived cloud and aerosol data meant to complement measurements from other A-train satellites, particularly Aqua and Cloudsat, which it closely follows in orbit (Winker et al. 2007). Since CALIPSO and MPLNET both observe backscatter from clouds and aerosols, their observations can be directly compared.

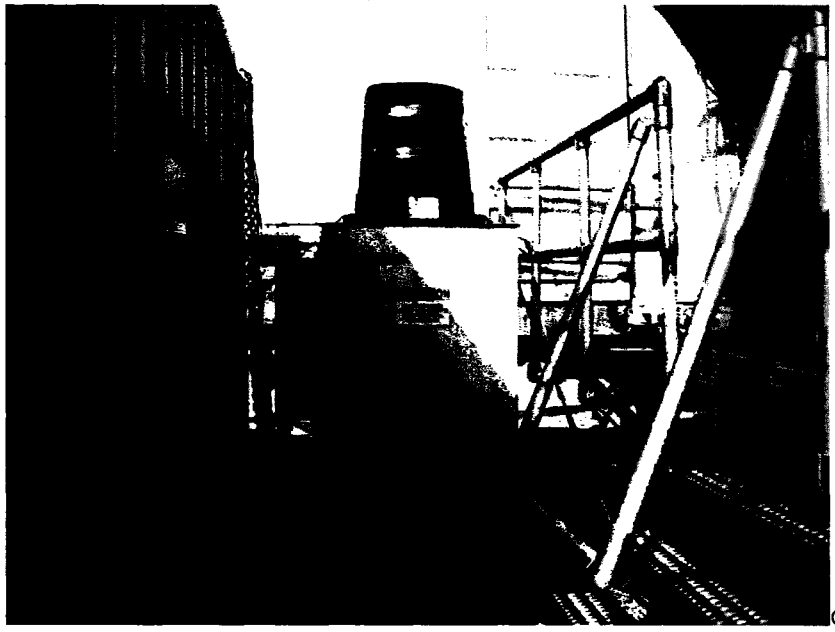
a)

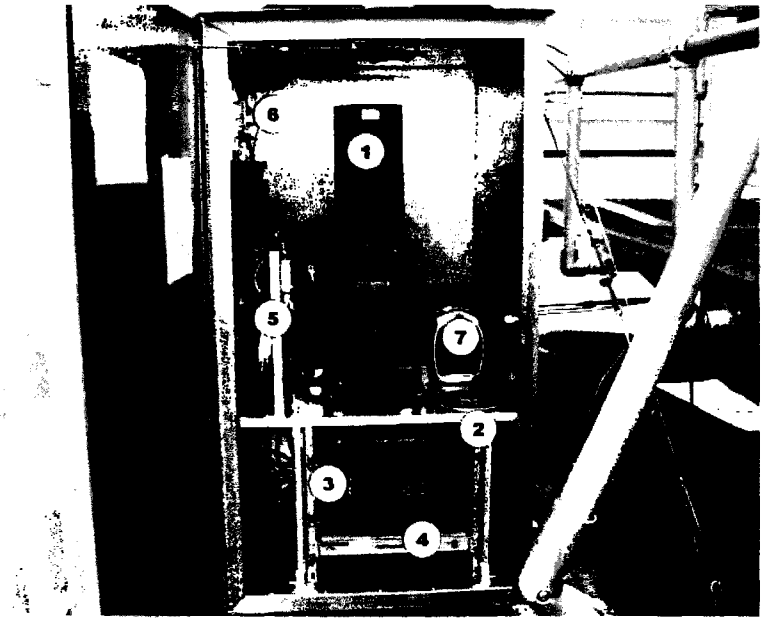

b)

Figure 3a. MPL412 in its enclosure aboard the *R/V Knorr*. The wastebasket provides an impromptu spray shield for the instrument window, which is therefore not visible; also note the radiation shield for a diagnostic temperature probe mounted on the left side of the enclosure, and the enclosure heater behind it. Figure 3b. Inside the enclosure. Parts include 1) telescope and detector, 2) control computer with Ethernet connection, 3) laser, 4) data system, 5) temperature probes for diagnostic purposes, 6) enclosure heater/air conditioner, 7) backup heater for extreme cold. The telescope is placed directly below a window in the enclosure. The control computer can be accessed remotely so that the enclosure seldom needs to be opened.

CHAPTER II

METHODS

An algorithm to automate PBL height detection must take advantage of the differences that appear in the aerosol backscatter profile between the mixed layer below the PBL and the free troposphere aloft. An idealized profile takes the form of a step function: backscatter is a constant with relatively high values for the lowest part of the atmosphere, and the abrupt change to lower backscatter values marks the PBL height. Davis et al. (2000) and Brooks (2003) recommend applying a wavelet covariance transform using the Haar function, as below:

$$W_f(a,b) = a^{-1} \int_{zb}^{zt} f(z) h\left(\frac{z-b}{a}\right) dz$$

where *f(z)* is the backscatter as a function of altitude, and the Haar function

$$h\left(\frac{z-b}{a}\right) = \begin{cases} -1 : b - \frac{a}{2} \le z \le b \\ 1 : b \le z \le b + \frac{a}{2} \\ 0 : elsewhere \end{cases}$$

In the Haar function, z is the altitude, *a* is the arbitrarily-chosen dilation of the step (ideally corresponding to the depth of the transition zone, such that the reported PBL height is the midpoint of the transition) and *b* is the translation factor. At the maximum of *Wf(a,b)*, the Haar function most resembles the backscatter profile, and *b* is the PBL height. With only slight modifications to

avoid mislabeling high clouds, this algorithm can find the PBL height automatically (Figure 4).

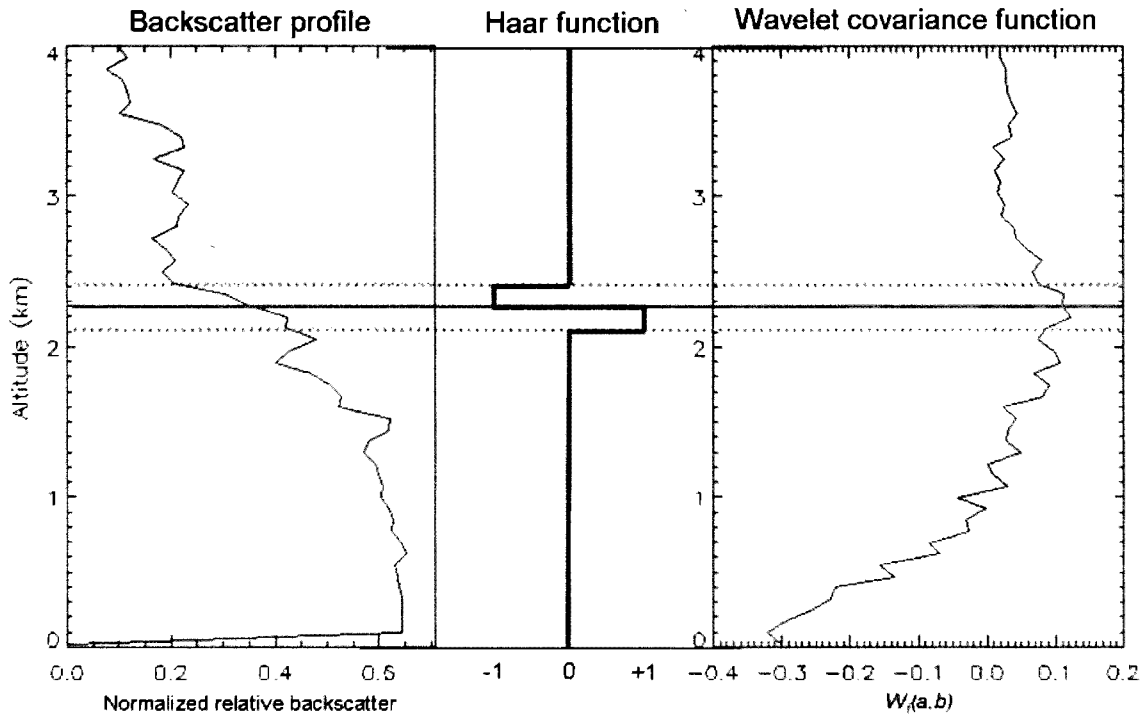

Figure 4. An example 1-minute backscatter profile, the matching Haar wavelet, and the wavelet covariance transform used to identify the planetary boundary layer height. The solid gray line marks the maximum of *Wf(a,b)*, while the dashed lines show the dilation *a* of the Haar function.

Two PBL height datasets were produced from the ICEALOT backscatter data, both using an algorithm based on the Haar wavelet covariance transform. The first was a product available from NASA MPLNET as level 1.5 data, and includes information about cloud and aerosol layers as well as the PBL height itself. PBL heights from this set included several outlier points where the algorithm erroneously marked an elevated cloud base or aerosol layer in the free troposphere, resulting in a calculated PBL height kilometers too high (Figure 5). After inspection of this data set and the raw backscatter, a second set of PBL heights was calculated, without considering cloud data and using only the

lowest 3 km of the atmosphere. This threshold greatly improved computational speed and eliminated any unrealistically high PBL data points. Because the wavelet covariance transform is sensitive to the length of the backscatter profile given, however, the second algorithm returned PBL heights that were often slightly different from the more realistic level 1.5b results (Figure 6).

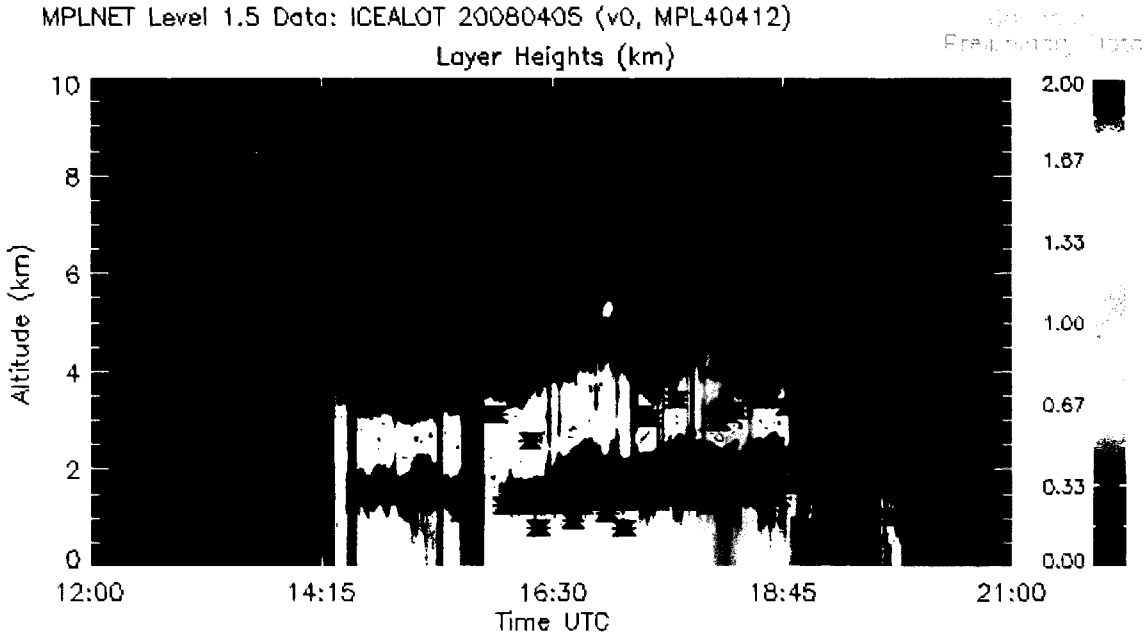

Figure 5. MPLNET backscatter data from 12:00 to 21:00 UTC, 5 April 2008 (see http://mplnet.gsfc.nasa.gov/data.html). Backscatter from cloud droplets is in white. The MPLNET level 1.5b data gives PBL heights above 2 km (black asterisks) for much of this period, but the true PBL height is near 1 km. The contrast in backscatter signal between the intensely reflective cloud droplets and the less reflective aerosol above it is high enough to mask the PBL signal from the wavelet covariance transform. With high clouds excluded from the algorithm, it returns better results.

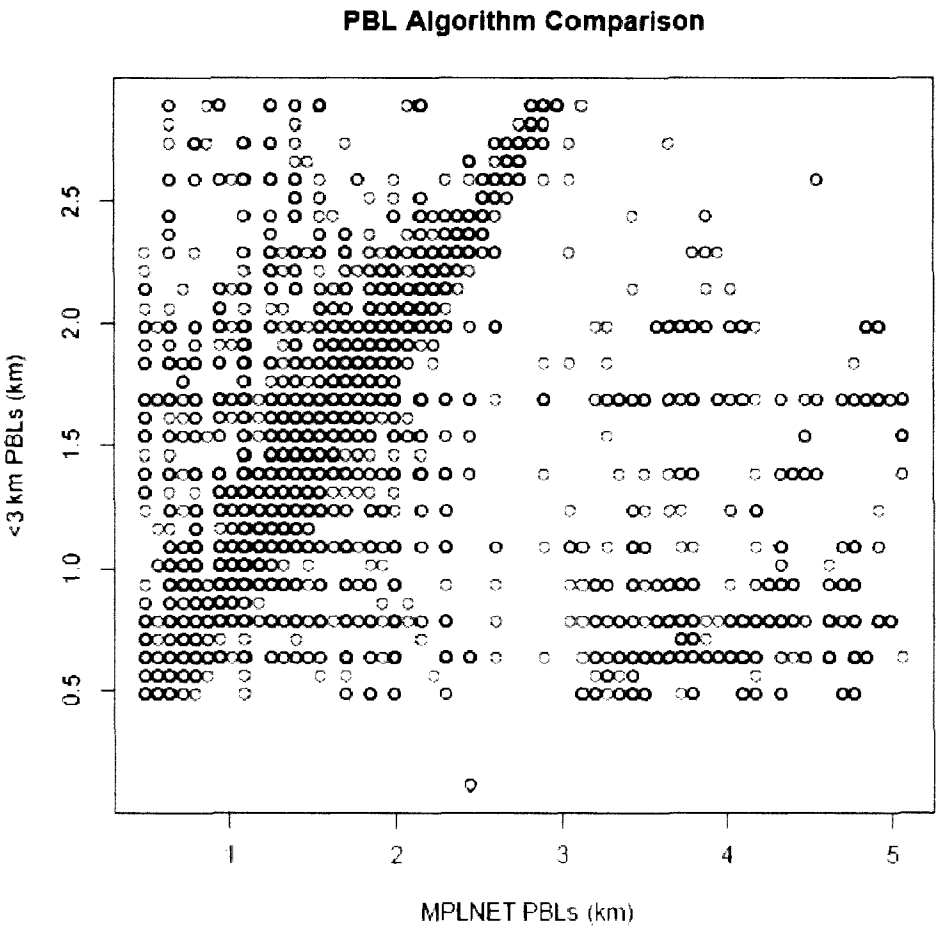

Figure 6. Comparison between PBL heights calculated by MPLNET for its level 1.5b data set vs. PBL heights calculated for the lowest 3 km of the atmosphere. Scatter beyond the downward adjustment of PBL heights above 3 km is due to the sensitivity of the wavelet covariance transform to the amount of data in the starting lidar backscatter profile, i.e. the depth of atmosphere for which the PBL is calculated.

Along with visual inspection of the lidar backscatter profiles and the resulting PBL calculations, verification of PBL heights using this method requires other observations in addition to the aerosol lidar. While most aerosol lidars in MPLNET are located at AERONET sites, allowing aerosol observations by multiple instruments at once, the ICEALOT lidar operated alongside several projects related to atmospheric chemistry, including balloon launches that yielded

upper-level meteorological data. Most important to PBL comparisons is the temperature observations taken by the sondes, which allow for direct observations of the PBL as opposed to proxy measurement by aerosol lidar. The PBL heights found using the Haar wavelet covariance transform as described above could therefore be compared to vertical temperature profiles from the same place and time. When the height identified by the wavelet covariance transform is within a low-level inversion in the temperature profile, it provides evidence in support of calculating PBL heights from aerosol lidar data.

In order to run statistical analysis comparing the PBL heights from the temperature profile to the heights derived from the lidar data, inversions were identified in the temperature profile first by finding data points with positive slope in temperature, and then by grouping these data points by height to distinguish between different inversions in the same profile. The total depth of the temperature inversion forms the transition zone, which may be up to several hundred meters deep. As the Haar wavelet covariance transform is intended to define the PBL as the center of the transition zone, the PBL heights taken from the sonde data are the mean heights of observations within the appropriate temperature inversion. The 83 resulting PBL heights were matched to the lidar PBL heights, averaged over the hour of the balloon launch to account for the time taken by the balloon's ascent. Both algorithms based on the wavelet covariance transform had a number of missing data points; there were 78 matches using the algorithm that considered only the lowest three kilometers of the atmosphere, and only 21 matches in the MPLNET level 1.5b dataset (Figure 7).

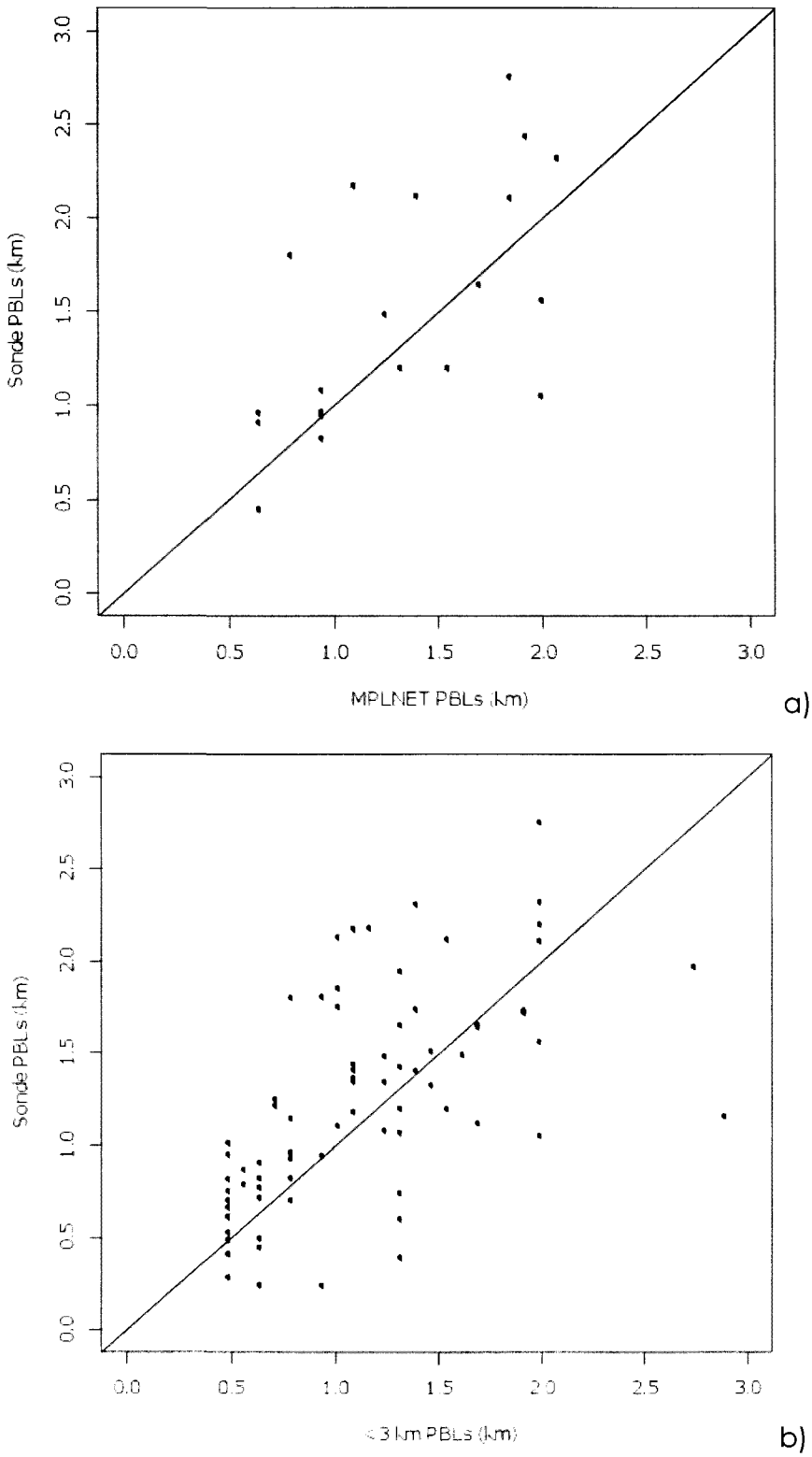

Figure 7a. Comparison between MPLNET PBL heights and PBL derived from sonde temperature profiles. Figure 7b. Between PBL heights calculated from the lowest 3 km of the atmosphere and the same sonde-derived PBL heights.

CHAPTER III

RESULTS

Comparison to Sonde Data

The root mean square error (RMSE) of PBL heights found using each of the two algorithms indicates the relative accuracy of the algorithms. The MPLNET level 1.5b data had a RMSE value of 0.820 km when compared to the PBL heights found from the balloon soundings. The RMSE of the newer algorithm was 0.497 km. The low RMSE values show that wavelet covariance transforms of aerosol lidar backscatter can provide a useful proxy for PBL height in the absence of direct measurements of temperature with height, as discussed in Davis et al. (2000) and Brooks (2003). Because of the smaller typical error and the much greater number of available data points, the PBL heights found using the newer algorithm will be used for analysis in the rest of the paper.

Because uncertainty exists in both the lidar-derived PBL heights and the heights found by visual inspection of the sonde temperature profiles, it is appropriate to compare the two sources of PBL data using an orthogonal regression or total least squares method. The resulting linear model has a slope of 1.072 and an intercept of 34.97 m (Figure 8), indicating a small bias that increases with higher PBL heights; lidar-derived PBL heights are consistently slightly lower in altitude than PBL heights found using the sonde temperature profile. The discrepancy is smaller than the depth of the bins used to group lidar backscatter by altitude; the accuracy of the method is therefore better than its precision.

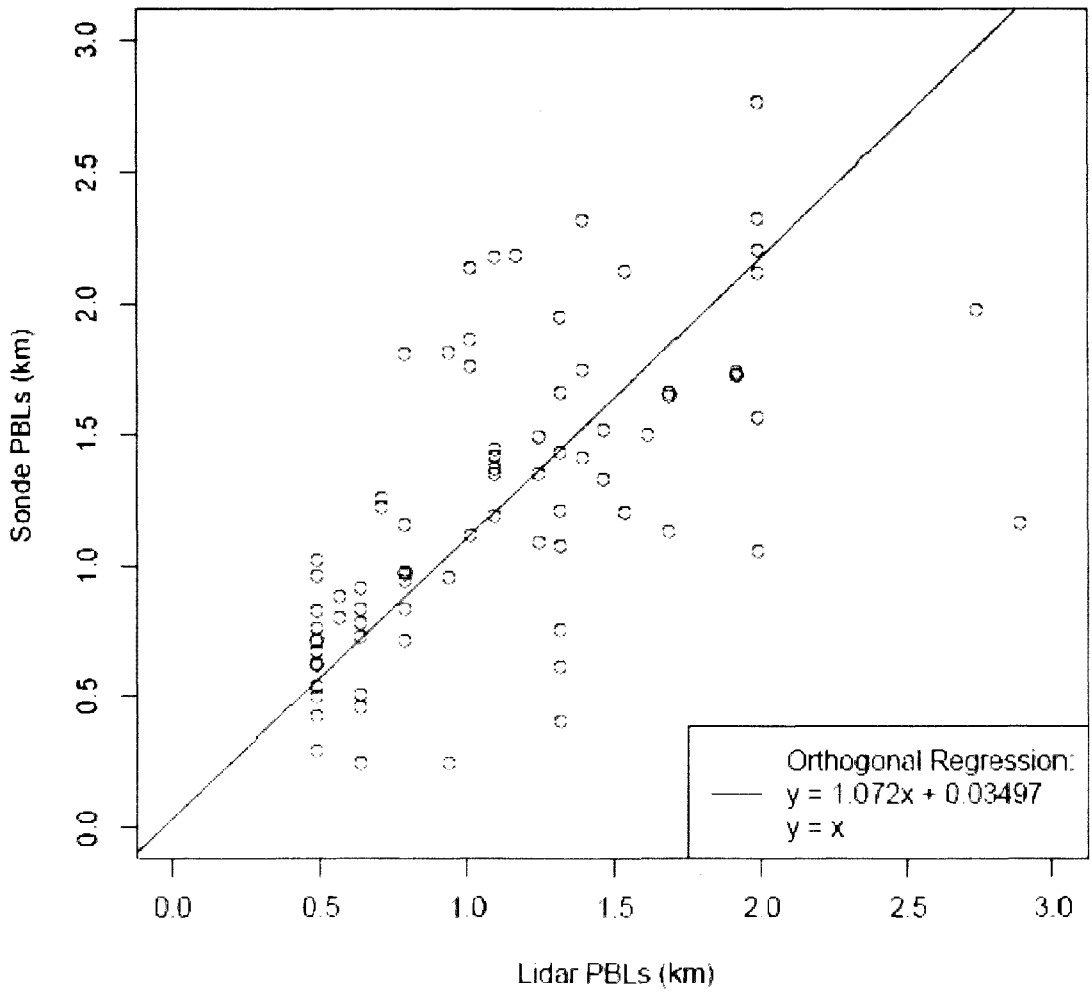

Figure 8. Orthogonal regression between lidar-derived PBL heights and sonde-derived PBL heights. The 1:1 line is shown in dotted gray for comparison.

Cruise Conditions

The PBL height varied over spatial as well as temporal dimensions as the cruise proceeded into the Arctic (Figure 9), and the weather varied considerably. For purposes of comparison, the record is divided into four periods corresponding to different geographical regions:

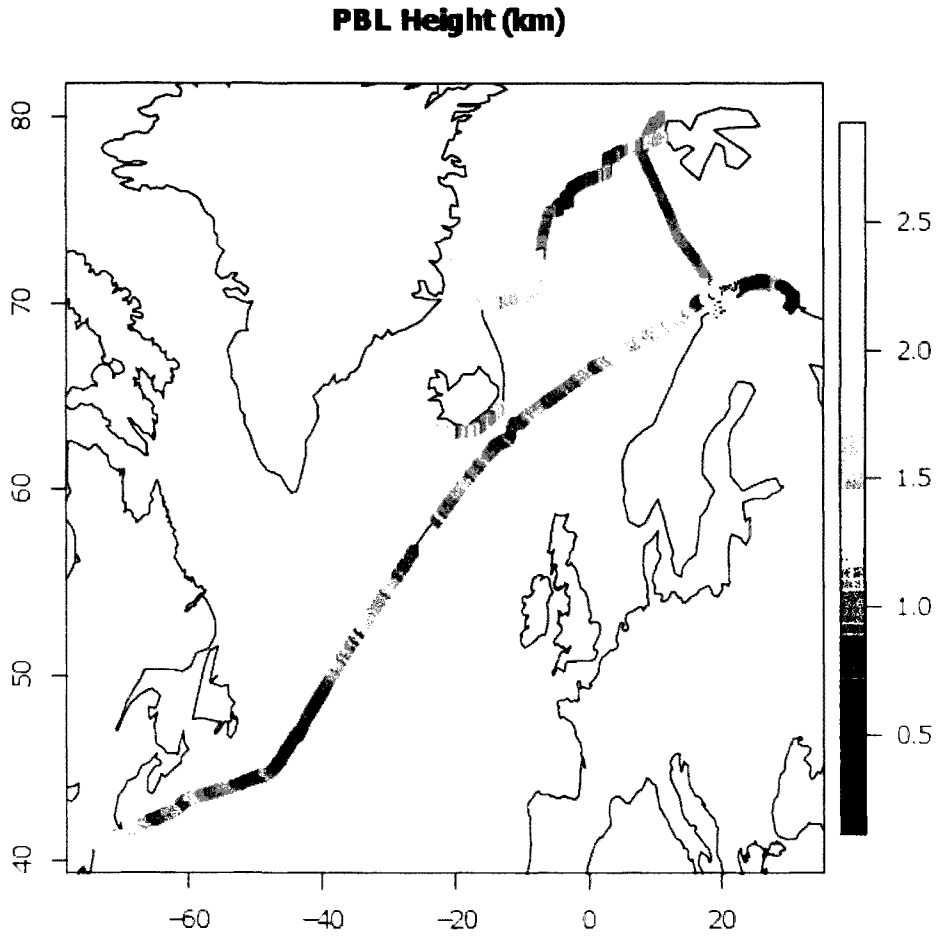

Figure 9. PBL heights by location, calculated using the Haar wavelet covariance transform over the lowest 3 km of the atmosphere.

The East Coast stage of the cruise took place 19 March 12:00 UTC to 25 March 21:00 UTC, and included observations of the coastline from Woods Hole, MA to the Long Island Sound, as well as a short stretch of continent-influenced air farther out to sea. The southernmost latitude reached during the cruise was 40.897° N, while the westernmost longitude was 73.696° W. Air temperatures were above freezing for this part of the cruise, sometimes as warm as 10° C, but sea surface temperatures hovered around 4-5° C. Winds were generally in the north.

The crossing of the North Atlantic formed the second stage of the cruise, taking place 25 March 21:00 UTC to 4 April 00:00 UTC. The weather became

stormy, and the *R/V Knorr* experienced the roughest seas of the cruise. Accordingly, the air temperature showed much less diurnal variability, while the wind speeds were consistently faster. The wind backed from 30 March to 2 April as the ship encountered a slow-moving low pressure center. Sea surface temperatures reached a high for the cruise of 14° C early in this period, and remained relatively warm. The PBL heights for the East Coast and North Atlantic crossing are plotted in Figure 10a.

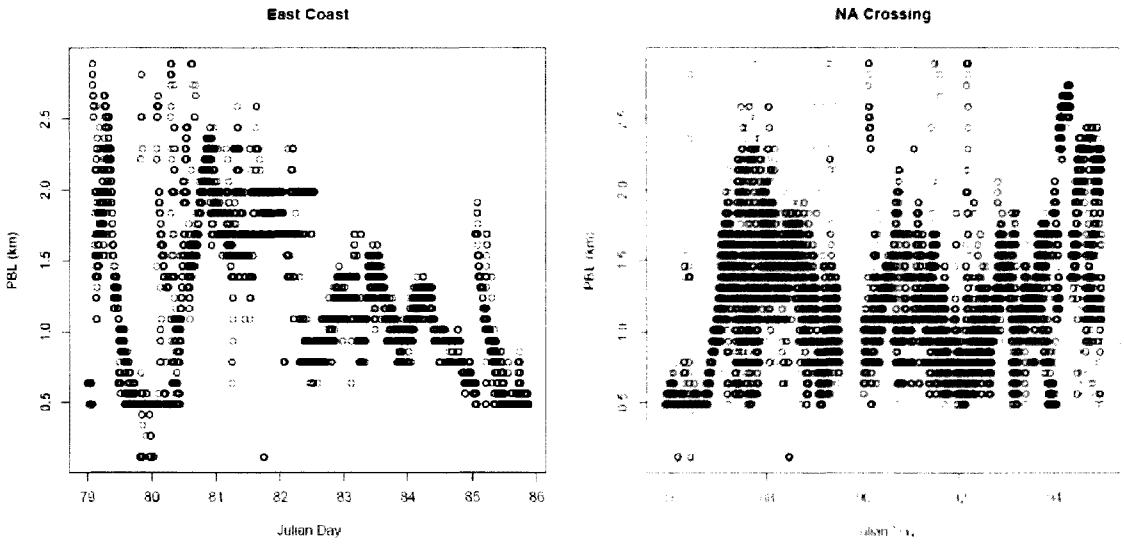

Figure 10a. Time series of PBL height during the first two stages of the cruise.

The third stage of the cruise is labeled Coastal Arctic. It took place 4 April 00:00 UTC to 14 April 08:15 UTC. The *R/V Knorr* traveled along the northern Scandinavian coastline to the Kola Peninsula, reaching the cruise's easternmost point at 31.530° E. The ship then turned westward and stopped at Tromsø, Norway. Fortunately for the cruise participants, the easterly winds were calmer than during the crossing. For the first time, air temperatures were sometimes colder than the sea surface, which dropped to 3° C.

The Far North stage of the cruise lasted until 23 April 16:00 UTC, when the lidar was shut down in preparation for the arrival of the *R/V Knorr* at Reykjavik, Iceland. The northernmost latitude reached during the cruise was 80.218° N. The coldest air temperature of the cruise was -16.9° C, falling on 16 April, but afterward it steadily climbed as the *R/V Knorr* headed southward, to 10° C and rain at Reykjavik. Sea surface temperatures dropped to near-freezing, but warmed on the last two days of the cruise to 8° C. Winds were variable in speed and direction. The PBL heights for the coastal Arctic and the far North are plotted in Figure 10b.

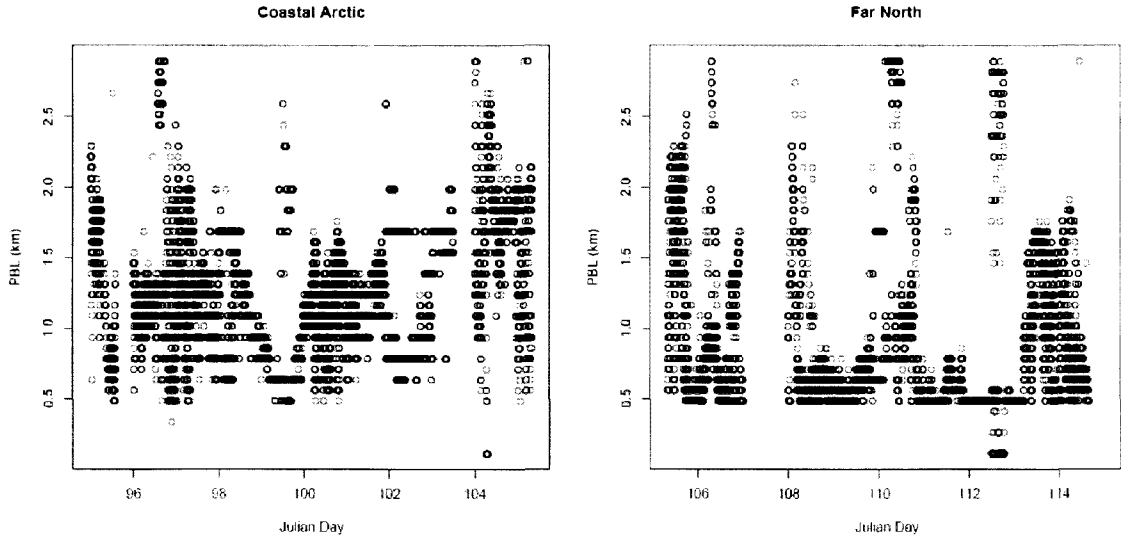

Figure 10b. Time series of PBL heights for the third and fourth stages of the cruise.

These differences in location and weather conditions contributed to the differences in the PBL height and its variability between stages of the cruise (Figure 11). However, the PBL height did not significantly correlate with any single meteorological variable as observed by the *R/V Knorr*, though Palm et al. (1996) predicted a relationship between PBL height and surface wind speed. One feature of the PBL record is common to the entire cruise: the absence of

afternoon convection due to surface insolation, which would have caused a rapid increase in the PBL height during daylight hours and a gradual decrease at night. The greater heat capacity of the ocean slows the re-radiation of sensible heat to the mixed layer, so the diurnal signal that is present in the PBL heights of land-based MPL stations does not appear in the cruise data. The difference in day length between the southernmost stage of the cruise and the far North therefore cannot be discerned from the diurnal variability.

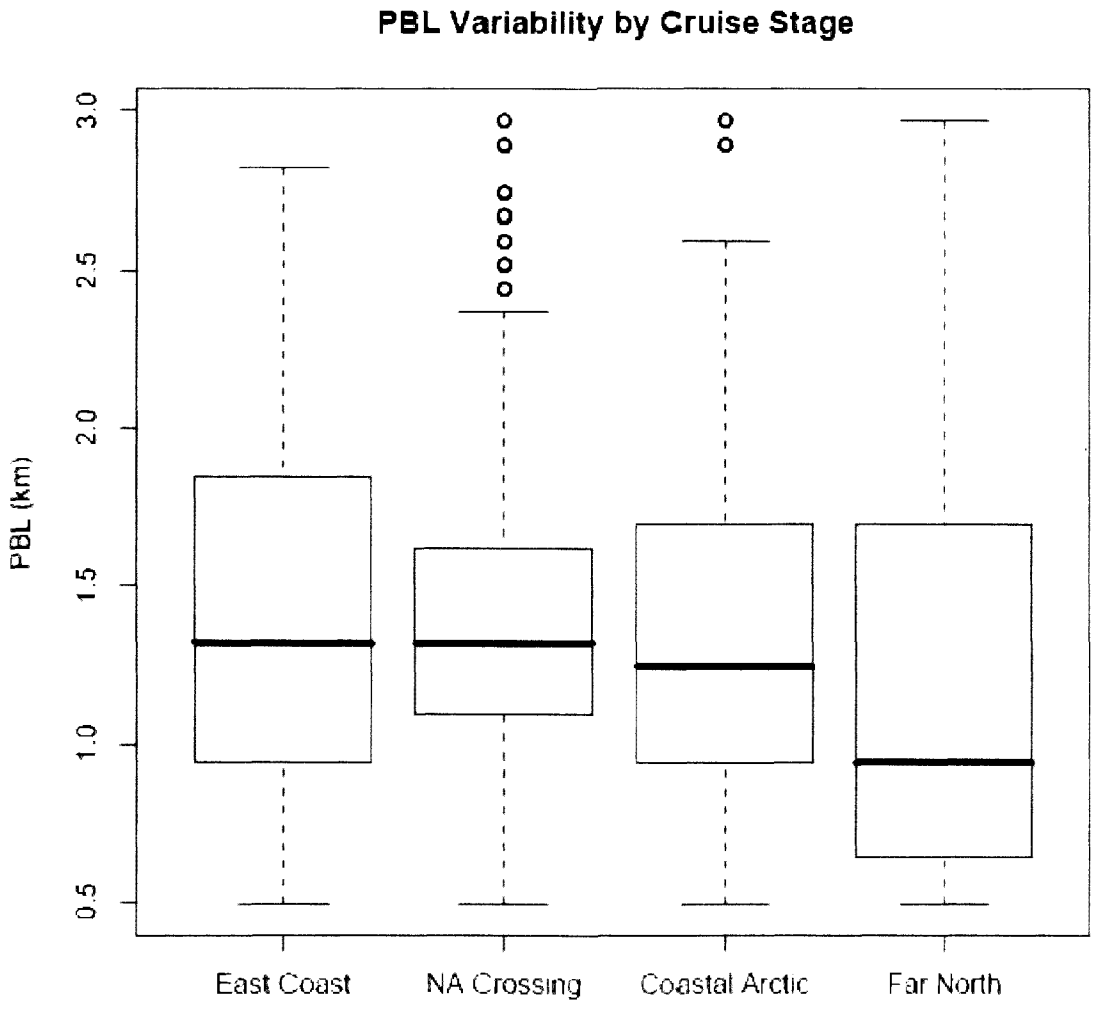

Figure 11a. Boxplots of PBL heights for different stages of the cruise.

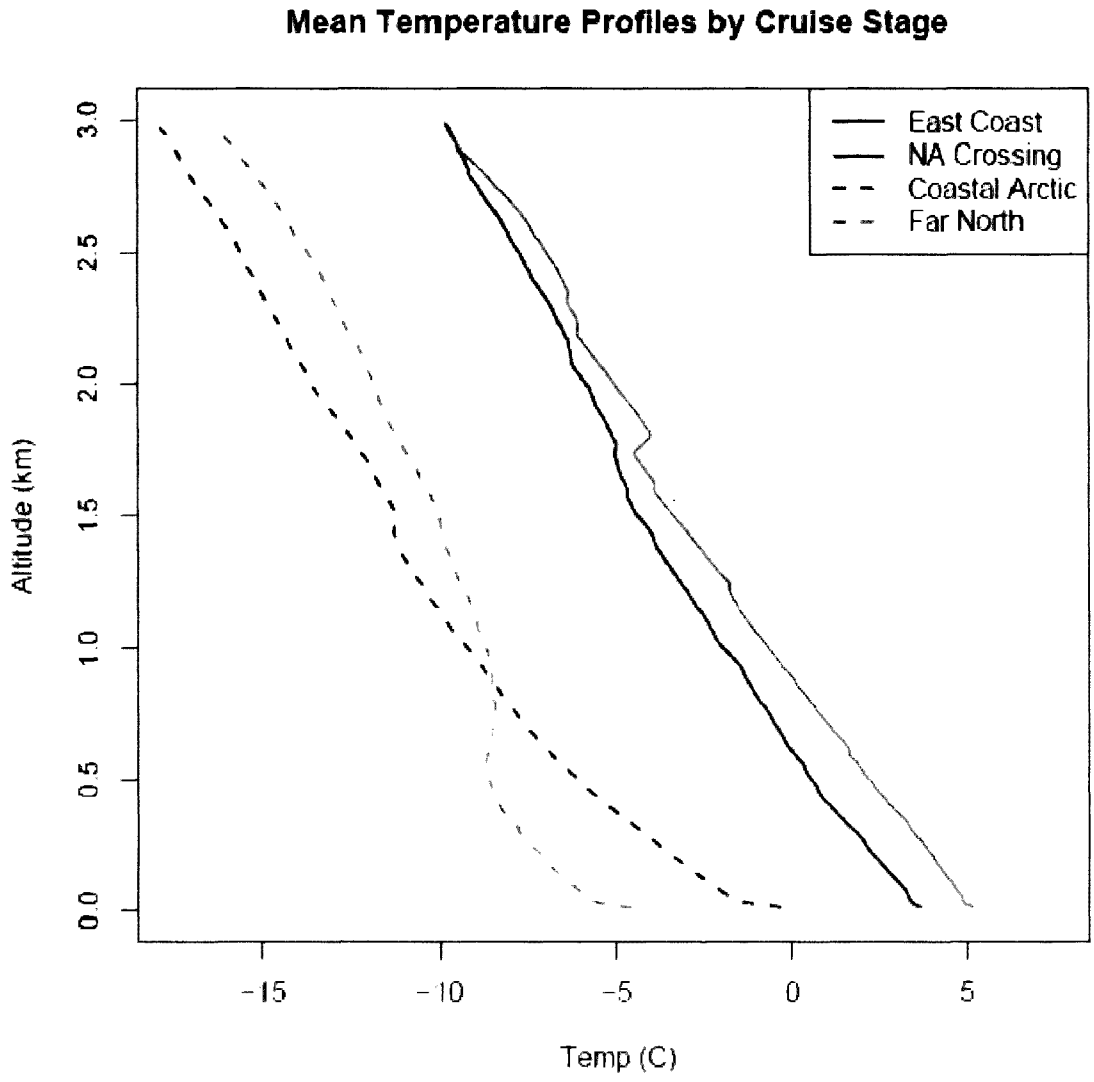

Figure 11b. Sonde temperature profiles averaged over each stage of the cruise. Colder temperatures and inversions at lower altitudes distinguish the northern reaches of the campaign.

CALIPSO Overpasses

The CALIPSO satellite passed over or very near the *R/V Knorr* four times during the course of the ICEALOT cruise. As a result, on four occasions the MPLNET lidar aboard ship was able to observe the atmosphere in the same time and location as CALIPSO's 532-nm aerosol lidar: one lidar ship-based and looking up, the other spaceborne and looking down. The resulting pairs of backscatter

profiles correspond only moderately, however (Figure 12). The first source of disagreement is noise and signal attenuation, which increase with distance from the lidar; thus when considering the lower troposphere where the PBL occurs, the MPLNET signal is at its strongest and clearest, while the CALIPSO data approaches its lowest signal-to-noise ratio. The second is due to cloud shadows: many clouds, especially those with low-level bases that often define the PBL, are opaque to aerosol lidar. CALIPSO is limited to observing aerosol above such clouds, while MPLNET only detects aerosol below them.

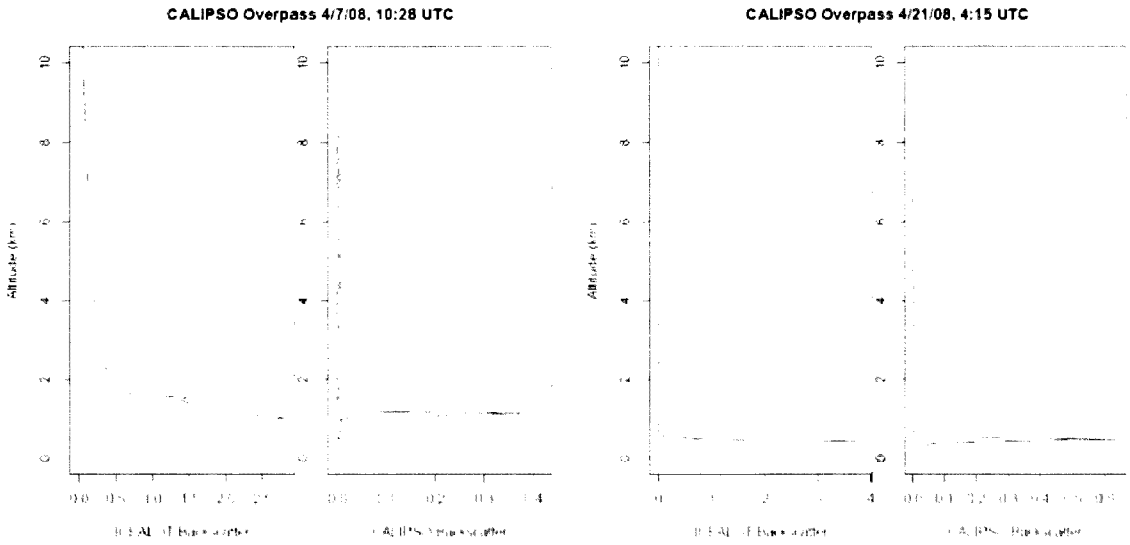

Figure 12. Side-by-side comparison of the backscatter data from MPLNET and CALIPSO during the overpasses of 7 April and 21 April. The first shows the signal from a cloud at PBL level, while the second is blocked by fog.

Overpasses occurred on 7 April, 11 April, 19 April, and 21 April, all north of the Arctic Circle. The middle two of these took place during significant events that are discussed below.

Forest Fires near Lake Baikal

On 11 April, the R/V Knorr approached Tromsø, Norway, and ICEALOT sampled surface air of Western European origin. However, HYSPLIT and FLEXPART

back-trajectory data shows that the prevailing wind at 5 km altitude was more northerly; the air mass aloft had crossed the pole since its last contact with the surface, and bore aerosol that was emitted in central Asia. The MPLNET lidar was able to detect a pronounced aerosol plume with several layers between 4 and 6 km altitude (Figure 13), which had first appeared at roughly 21:00 UTC on the night of 10 April. The crew of the POLARCAT France flight that passed over the ship during the morning of the 11th reported high concentrations of aerosol with a composition that suggested biomass burning, accompanied by carbon monoxide gas. As the day progressed, the biomass burning plume descended. The thickest part of the plume was at 3 km altitude by the evening of 11 April, and by mid-morning the next day it had crossed the PBL and entered the mixed layer.

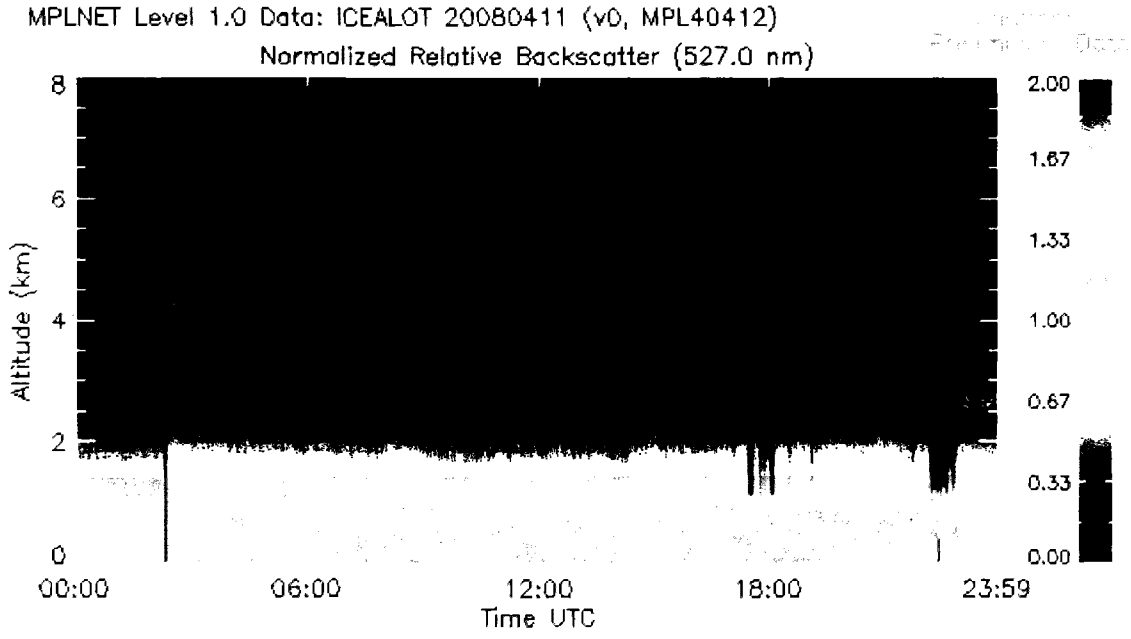

Figure 13. MPLNET backscatter signal for the entire day of 11 April 2008 (see http://mplnet.gsfc.nasa.gov/data.html). The PBL remains below 2 km throughout. The instrument was shut down briefly at 2:20 UTC in order to clean the window lens.

The CALIPSO overpass of 11 April occurred at 1:58 UTC, when the biomass burning plume was clearly visible in the MPLNET backscatter as a single layer at approximately 4.5 km. For comparison, the one-minute backscatter profile corresponding to the overpass was matched with the CALIPSO backscatter from the moment the satellite crossed the track of the *R/V Knorr* (Figure 14). Despite a much greater proportion of noise in the CALIPSO data, as discussed earlier, it was also able to detect a slight increase in aerosol reflectivity at the altitude of the biomass burning plume. As there were no clouds until late in the day, both lidars were able to observe the entire depth of the mixed layer and the atmosphere above it.

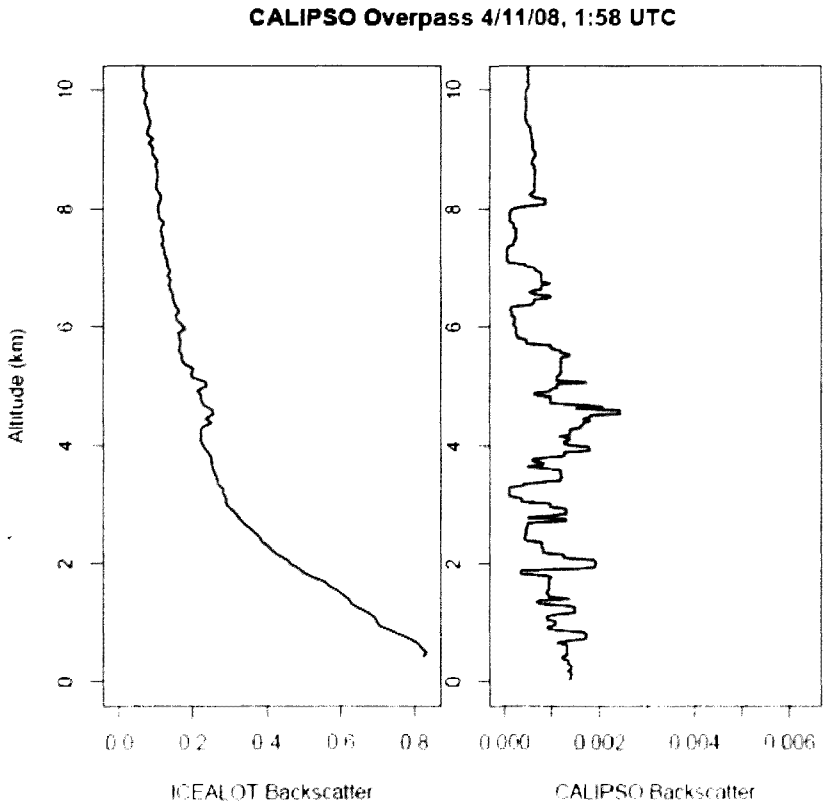

Figure 14. Side-by-side comparison of the backscatter data from MPLNET and CALIPSO during the 11 April overpass. A running median filter has been applied to the CALIPSO data; actual signal is in gray. The biomass burning plume appears between 4 and 6 km altitude.

The plume corresponds temporally to observations made in Alaska during ARCPAC. The biomass burning plumes observed by Warneke et al. (2009) came partly from forest fires near Lake Baikal in southern Siberia, and partly from agricultural fires in Kazakhstan to the west. MODIS photographed widespread fires in the area near Chita, Russia (approximately 52°N 113°E) and the Lake Baikal area from 7 April to 28 April, 2008 (Figure 15). The FLEXPART and HYSPLIT models indicate these forest fires as the most likely source of the plume observed during ICEALOT, as well as many of the plumes observed by Warneke et al. The area is subject to seasonal forest fires, but in most years the burning begins too late—generally at the end of April—to contribute to the Arctic haze. In 2008, however, low seasonal snowfall totals caused the fire season to begin during the peak of the Arctic haze.

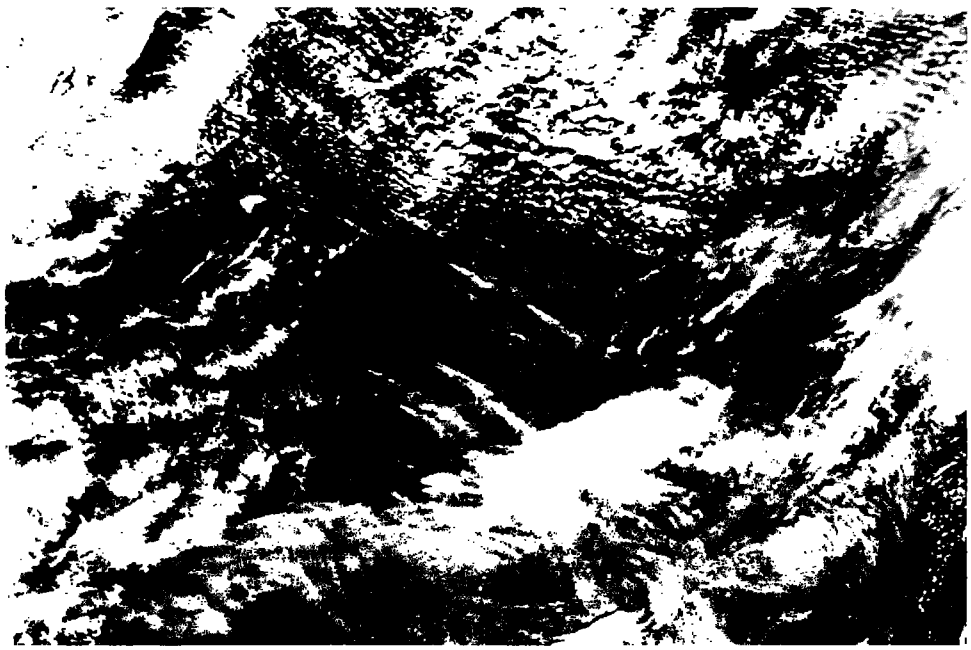

Figure 15. MODIS imagery of the fires near Chita, Russia. Smoke plumes in the center of the image are darker than the surrounding clouds and flow southeastward. Source: NASA Earth Observatory, http://earthobservatory.nasa.gov/NaturalHazards/

Invisible Clouds?

19 April brought the *R/V Knorr* across the Prime Meridian headed southwestward, close to the ice edge off the coast of Greenland. The path of CALIPSO came close to the ship's track at 4:25 UTC, but never crossed it; the resulting pair of profiles is therefore taken from slightly different locations (Figure 16). This serves to explain the mismatch in the signal at 6 km, where the MPLNET lidar detected cirrus cloud but the CALIPSO profile had no corresponding peak (Figure 17). The weather was mostly clear to the eye, with only a few scattered cirrus clouds, so the difference in the signal over short horizontal distances is not surprising.

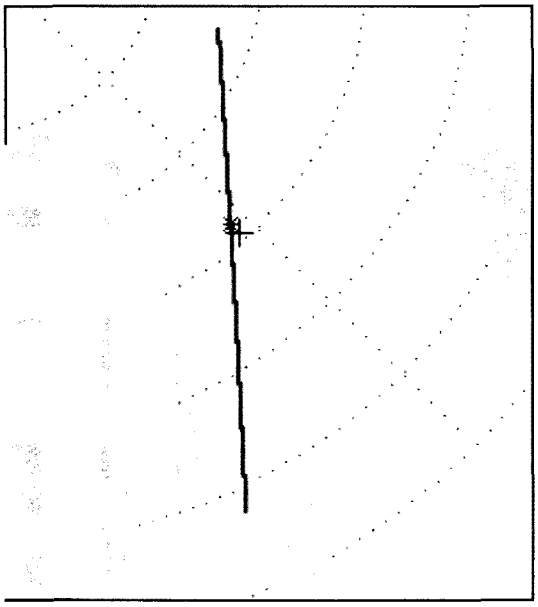

Figure 16. The position of the *R/V Knorr* on 19 April at 4:25 UTC, marked with a plus sign, and a short segment of CALIPSO's track from the same period, marked with a solid black line. The asterisk on the line marks the location of the CALIPSO backscatter profile closest to the ship's position. This is considered the "overpass" profile, but it is approximately 52 km from the location observed by the matching MPLNET profile. For the other three overpasses, the track of the *R/V Knorr* truly intersected with the path of CALIPSO, and the match in location is much more exact.

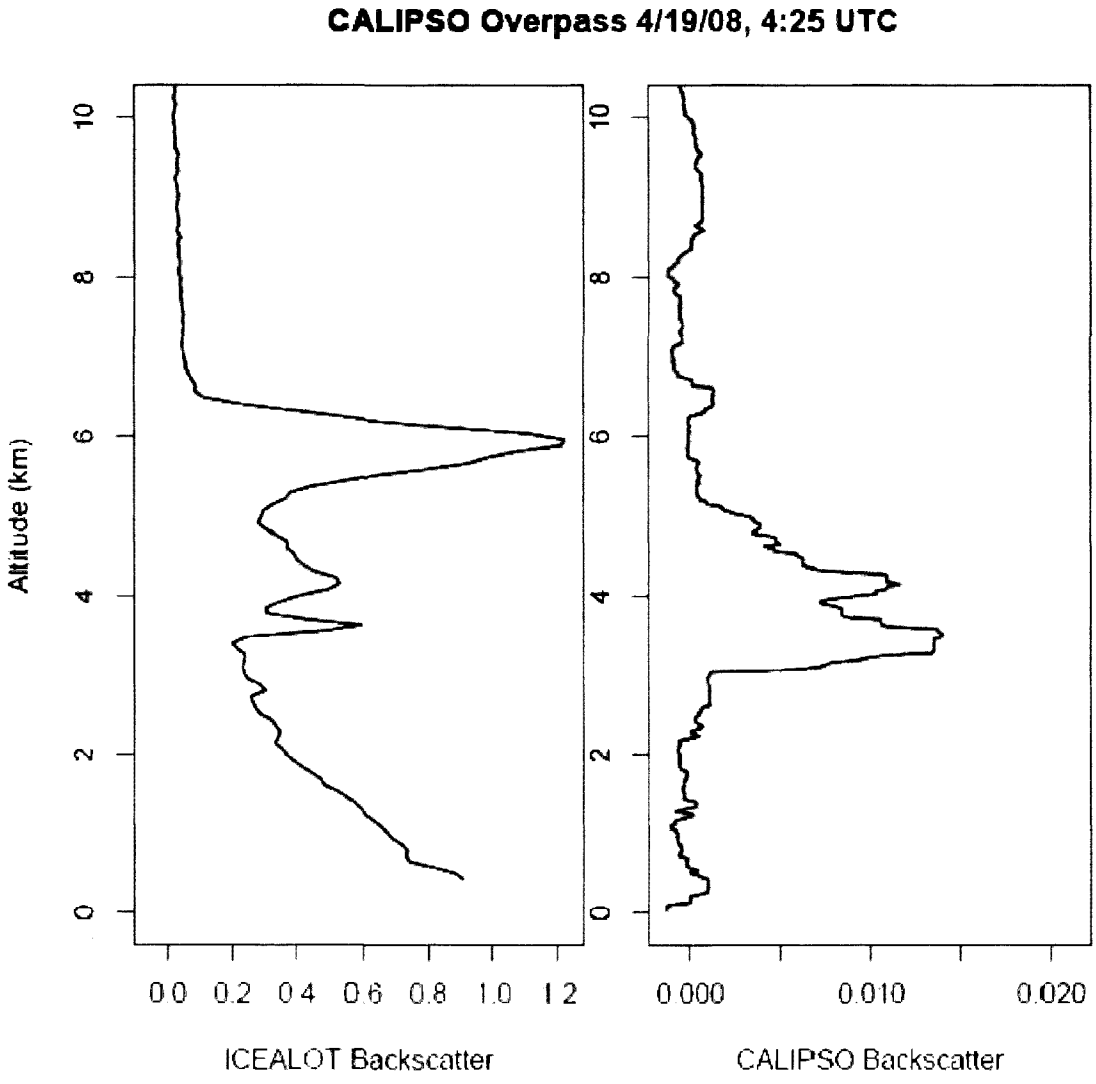

Figure 17. Side-by-side comparison of backscatter profiles for the 19 April near-overpass. Again, the CALIPSO data is in gray with a running median plotted on top.

However, the patchy cirrus deck was not the only feature the lidars observed. At approximately 3-5 km there was a backscatter signal consistent with thin ice cloud. For neither lidar was it opaque enough to cast a shadow on the opposite side of the profile, but both show a strong peak in the backscatter at that altitude. Looking at several hours' worth of data observed by the MPLNET lidar (Figure 18), the structure of the feature includes slanted vertical lines of

bright reflectivity, the kind that Shiobara et al. (2003) attribute to large, falling ice crystals within a cloud.

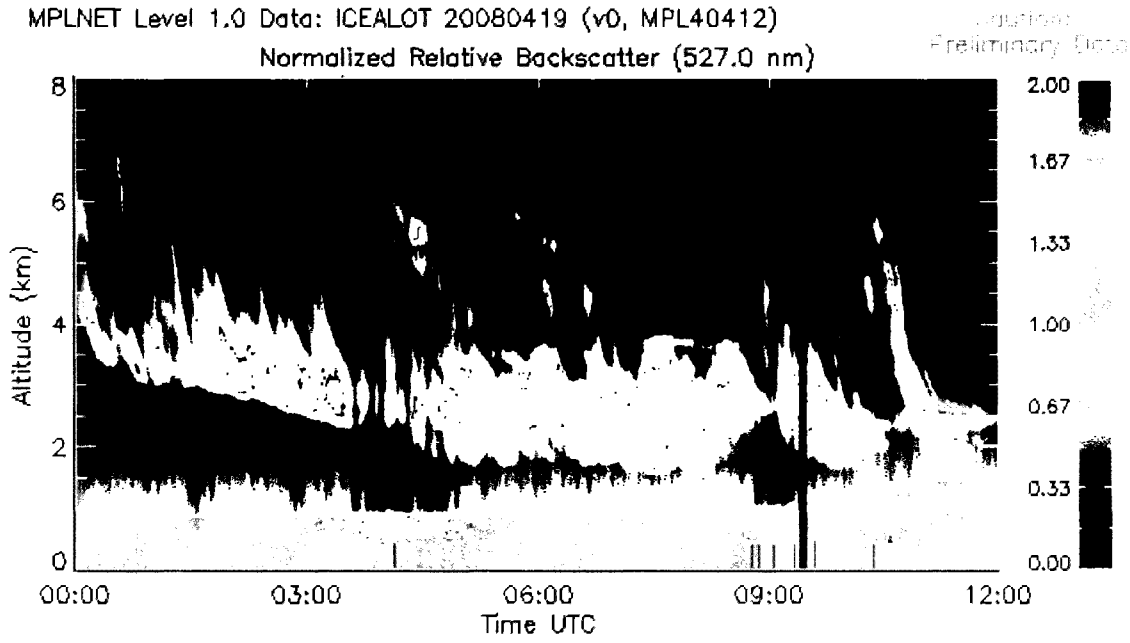

Figure 18. MPLNET backscatter signal for the morning of 19 April 2008 (see http://mplnet.gsfc.nasa.gov/data.html).

To an unaided observer on the deck of the *R/V Knorr*, this apparent cloud deck was not visible. Aside from its cloud-like structure and high reflectivity, the feature could not be an unusually bright aerosol layer, because HYSPLIT back-trajectories showed no single near-ground origin for the air at that altitude. Air within the apparent cloud deck was last in contact with the surface on either Baffin Bay or the Greenland Sea, at times varying from three to ten days prior to 19 April. Most likely, the feature is indeed an ice cloud, made up of unusually large ice crystals, but too diffuse to be visible to a human observing sky conditions by eye. This idea is further supported by the fact that lower cloud layers gradually filled in the sky later in the day, as might be expected after the

observation of widespread cirrus. By the evening of 19 April, the *R/V Knorr* was once again under fog.

Continental Aerosol off the Long Island Coast

Early in the cruise on 22 and 23 March, the *R/V Knorr* traveled eastward. Although the end of this two-day period brought the ship more than a thousand kilometers from land, the air mass that the instruments sampled was continental in origin—back-trajectories from HYSPLIT show a northwesterly path out of Canada. Accordingly, although the air was clean by continental standards, the aerosol backscatter signal was still higher than at many other points during the cruise. The most recognizable feature in this period was a layer of aerosol that rode several hundred meters above the PBL, at around 3 km altitude (Figure 19).

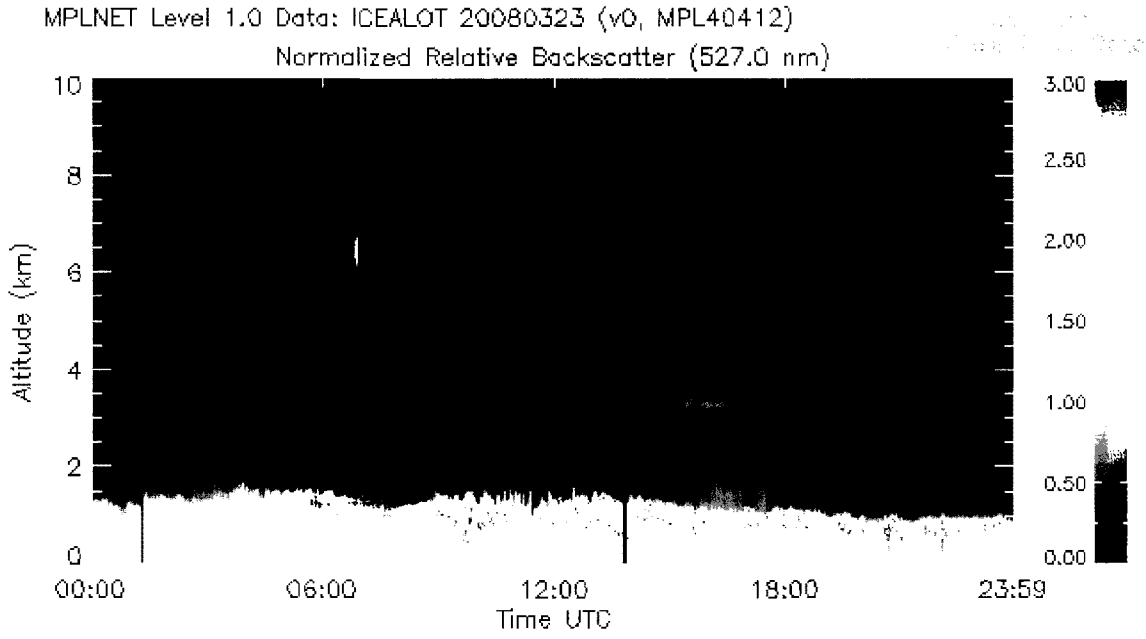

Figure 19. MPLNET backscatter signal for 23 March 2008, during ICEALOT.

The HYSPLIT back-trajectory shows that this elevated aerosol layer had crossed the coastline roughly six hours earlier. It must have been regionally widespread, because the same layer appeared in the backscatter signal from

another MPLNET lidar that was situated permanently at Thompson Farm in Durham, New Hampshire (43.11° N, 70.95° W). The layer is slightly more elevated in the Thompson Farm record, and it dissipates not long after 12:00 UTC (Figure 20). This is consistent with the hypothesis that both lidars observed the same aerosol layer at different times during the day, as it was transported eastward across the Northeast region of the United States and out to sea.

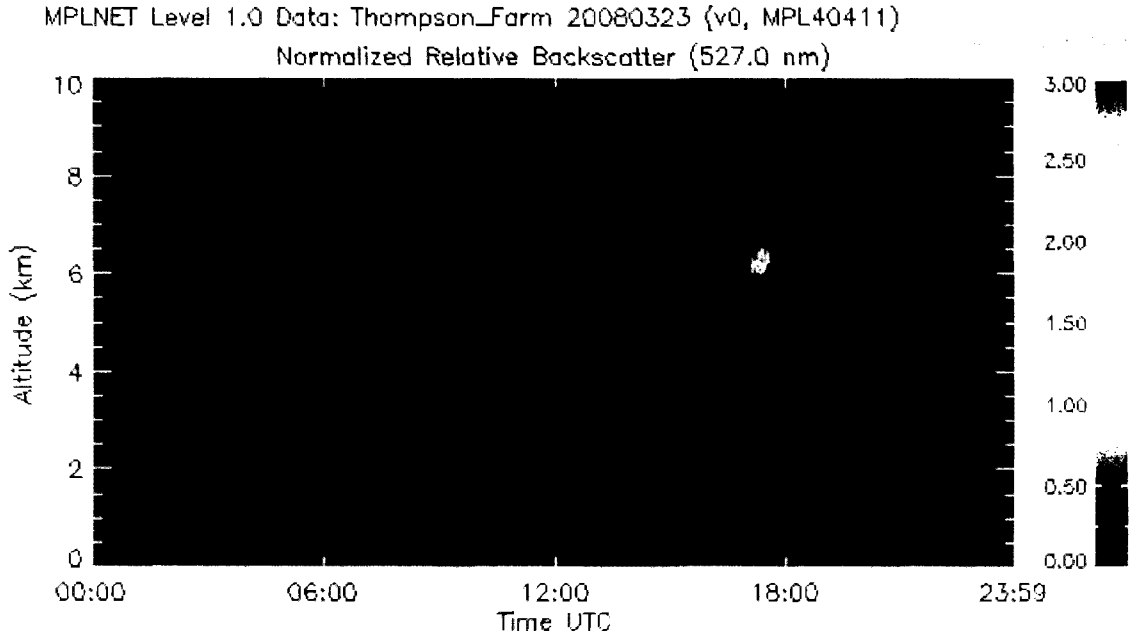

Figure 20. MPLNET backscatter signal for 23 March 2008, at Thompson Farm.

The mixed layer at Thompson Farm has a dimmer backscatter signal than that observed by the ICEALOT lidar, but this does not necessarily indicate a difference in aerosol concentration. In their preliminary data, MPLNET lidars observe relative backscatter only; the conditions of the laser and telescope vary from one location to the next, making direct comparison between instruments impossible. However, the elevated aerosol layer that appeared as a feature in both retrievals shows that the same airmass passed over Thompson Farm and the *R/V Knorr* (Figure 21).

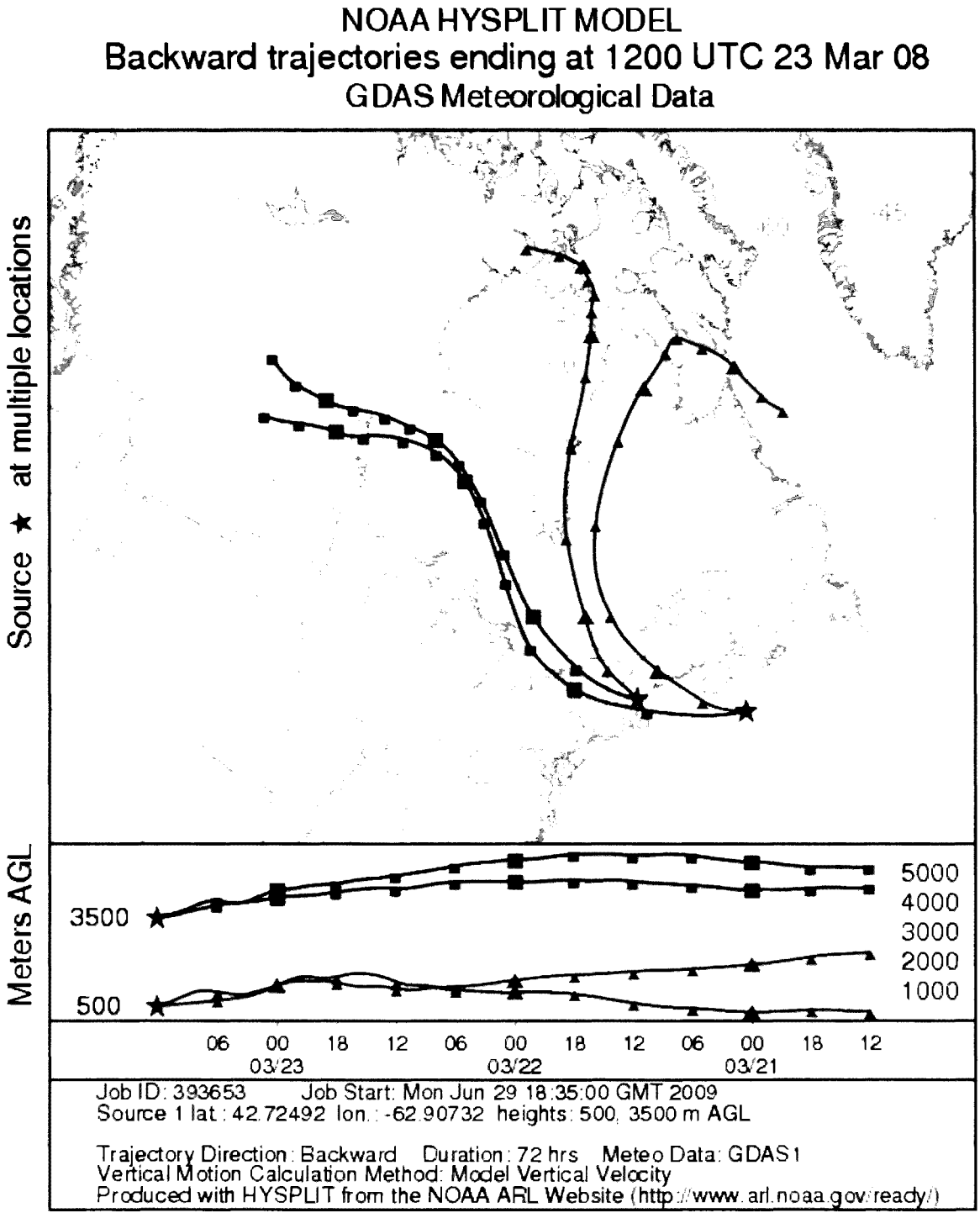

Figure 21. HYSPLIT back-trajectories for Thompson Farm and ICEALOT at 12:00 UTC, 23 March 2008. While the air at 3500 m has the same source at both stations, the air below the PBL is more varied on a regional scale.

CHAPTER IV

DISCUSSION

The simplest technique for PBL detection in aerosol lidar backscatter involves setting thresholds for changes in backscatter intensity (Melfi et al. 1985, Palm et al. 1998). A correctly developed threshold can detect the pronounced drop in aerosol concentration at the transition from the mixed layer to the free troposphere, but it cannot be generalized for different sites and atmospheric conditions. Parikh and Parikh (2002) took a different approach by formatting the backscatter data as an image file, and applying edge detection methods. While it requires greater knowledge of underlying features in the data to distinguish the PBL from cloud shadows and other structures, this method is undoubtedly an elegant way to detect PBL heights in large data sets. The wavelet covariance transform used in this paper is described in Brooks (2003) and Davis et al. (2000) as a refinement of the threshold method, with the additional ability to detect the PBL as a transition zone of variable depth rather than as a discrete height.

Because the ocean surface responds slowly to insolation, there is little diurnal variation in the marine PBL height. This effect is exacerbated in the Arctic, where surface convection is rare due to cold temperatures, and the atmosphere is often very stable. Still, even well north of the Arctic Circle, the PBL heights observed during the cruise varied from a few hundred meters to almost 3 km. The PBL varied in altitude and distribution during the different stages of the cruise, but

a relationship to surface wind speeds, latitude, or static stability could not be generalized. Relationships between these factors and PBL height expressed in Holton (2004) and Peixoto and Oort (1992) are not apparent in the data. Though the relatively uniform ocean surface seems to eliminate many of the small-scale dynamics that complicate prediction on land, caution must be exercised in estimating PBL from one or two meteorological variables.

Palm et al. (1996) observed a correlation between the surface wind speed over the ocean and the PBL height that accompanied it. This was explained by the equation for latent heat flux

$$E = L_v C_e U \rho (q_s - q)$$

with latent heat of vaporization L_v, air density ρ, transfer coefficient C_e, and the difference between saturation specific humidity for a given SST and actual specific humidity $q_s - q$. U is then the mean wind speed at 10 m; as the PBL height is often determined by the strength of the latent heat flux from the ocean surface, a relationship to the wind speed could be expected as long as latent heat transfer dwarfed other variables. This assumes a small difference between air temperature and SST, however, which is seldom the case in the parts of the Arctic kept ice-free by the Gulf Stream.

The four CALIPSO overpasses demonstrated the strengths and limitations of satellite-based aerosol lidar in the Arctic, compared to ground-based methods. If the day was mostly clear or had cloud decks at the cirrus level, even widespread cirrostratus like the layer on 19 April, there was good correspondence between the ship-based lidar backscatter profile and the CALIPSO profile of the same time and location; the main problem was the low

signal-to-noise ratio of the CALIPSO profile at the limits of its range, which may respond to filtering techniques. However, on the two overpasses that occurred when low clouds were present, CALIPSO failed to retrieve data from below the cloud top, missing the PBL and mixed layer entirely. In cases of fog or moderate to heavy precipitation, the MPLNET lidar was similarly blocked. In other cases, such as fair-weather cumulus or a dense stratus deck, the ship-based lidar returned a profile of the mixed layer without difficulty, and was only blocked from the free troposphere above the cloud deck.

It is important to note that the forest fires of the Lake Baikal region affected an area 4,800 km from the 11 April position of the *R/V Knorr*, where soot and other products of the fires were detected. This aerosol became part of the Arctic Haze for the 2008 season, crossing the Arctic as an elevated layer in the free troposphere but later dropping through the PBL and into the mixed layer. Anthropogenic components of the Arctic haze have often traveled similar distances. Such long-range transport is only possible above the PBL, where turbulence and vertical motion occur on a much smaller scale than the geostrophic flow of free tropospheric winds.

The MPLNET lidar aboard ICEALOT provided one of relatively few sources of data about the elevated aerosols and clouds associated with the Arctic haze. The case study of 19 April, in which a cirrostratus deck was invisible to ground observers but not to the lidar, proves that the continuously-operating lidar can even improve the accuracy of meteorological observations. The biomass burning plume of 11 April showed the importance of observations at the PBL and above; the airmass at the surface arrived on a southerly wind with European

origins, while 4 km overhead, the signs of an Arctic haze event were clear more than 24 hours before the plume entered the mixed layer.

Because such a large proportion of anthropogenic aerosols in the Arctic enter the region after traveling long distances in the free troposphere, better data on the PBL and the troposphere above it can improve understanding of Arctic air pollution in general. The sources of aerosol are limited to plumes that escape the PBL in the midlatitudes and enter the free troposphere. In the Arctic, mixing through the PBL determines how much of these aerosols affect the surface, and how quickly they can be removed from the atmosphere. Due to the lack of diurnal variation in the PBL height and the relatively weak convection that occurs over the Arctic Ocean, the most common mechanisms for entrainment from the free troposphere into the mixed layer are minor effects. Further research is needed to understand the processes that allow this mixing to occur during Arctic haze events.

CHAPTER V

CONCLUSIONS

During ICEALOT, the aerosol lidar aboard the *R/V Knorr* operated continuously with a one minute temporal resolution. The resulting backscatter signal contains information about cloud layers, aerosol concentrations, and the height of the PBL throughout the cruise. The RMSE value for these PBL heights is approximately 500 m, making them an effective supplement to the PBL information that can be found in sonde data (up to four launches per day during ICEALOT). While the PBL height as a single number per time step does not convey information about the depth of the transition zone or the strength of the inversion, it is available on short enough time scales to watch changes develop over a matter of hours. In addition, the same algorithm can be applied to backscatter data from the CALIPSO satellite; while the results are less reliable due to cloud opacity and the distance of the satellite from the PBL, CALIPSO could potentially provide spatial coverage of PBL heights that would be impossible for any ground-based method, especially over the ocean. For purposes of comparison with MPLNET using the four CALIPSO profiles that occurred during overpasses of the *R/V Knorr*, a running-median filter was sufficient to distinguish features from the noise in the data. Further work would be needed to determine if smoothing techniques could be useful in PBL detection with CALIPSO alone.

The wavelet covariance transform technique successfully detected PBL heights in an ice-free part of the Arctic Ocean, where conditions are very

different from the land-based, midlatitude sites for which the algorithm was originally developed. Diurnal variation in the PBL from insolation-driven atmospheric convection is nearly absent in the cold marine environment; entrainment of elevated aerosols trapped in a rising PBL does not appear to occur. Other mechanisms must dominate mixing from the free troposphere through the PBL and into the mixed layer below. The frequent fogs and low cloud decks of the springtime Arctic are a more likely cause of changes to PBL height in the region, but more research is required to determine whether these weather events replace the role of convection in atmospheric mixing.

Automated PBL detection in aerosol lidar backscatter is a vital tool in understanding the chemistry of the lowermost kilometers of the atmosphere. Methods that observe the PBL directly, with vertical temperature and humidity profiles, are difficult to obtain with sufficient spatial and temporal coverage to monitor the development of changes in the PBL on scales comparable to the weather conditions that cause them. The behavior of the PBL has implications for atmospheric chemistry and global climate, especially in coastal and marine environments and in remote regions such as the Arctic, where long-range transport of pollutants determines a large part of the composition of air pollution.

LIST OF REFERENCES

Brooks, Ian M., 2003. Finding boundary layer top: application of a wavelet covariance transform to lidar backscatter profiles. *J. Atmos. Oceanic Technol.* 20, 1092-1105.

Campbell, James R., et al., 2002. Full-Time, Eye-Safe Cloud and Aerosol Lidar Observation at Atmospheric Radiation Measurement Program Sites: Instruments and Data Processing. *J. Atmos. Oceanic Technol.* 19, 431-442.

Davis, K. J., et al., 2000. An objective method for deriving atmospheric structure from airborne lidar observations. *J. Atmos. Oceanic Technol.* 17, 1455-1468.

Heidam, Niels Z. et al., 2004. Arctic atmospheric contaminants in NE Greenland: levels, variations, origins, transport, transformations and trends 1990–2001. *Science of the Total Environment* 331, 5-28.

Holton, James R. *An Introduction to Dynamic Meteorology*. 4th ed. Boston: Elsevier, 2004.

IPCC, 2007. *Climate Change 2007: The Physical Science Basis. Contribution of Working Group I to the Fourth Assessment Report of the Intergovernmental Panel on Climate Change* [Solomon, S., D. Qin, M. Manning, Z. Chen, M. Marquis, K.B. Averyt, M. Tignor and H.L. Miller (eds.)]. Cambridge University Press, Cambridge, United Kingdom and New York, NY, USA.

Law, Kathy S. and Andreas Stohl, 2007. Arctic air pollution: origins and impacts. *Science* 315, 1537.

Melfi, S.H., et al., 1985. Lidar observations of vertically organized convection in the planetary boundary layer over the ocean. *J. Climate Appl. Meteor.* 24, 806-821.

Mitchell, J. M. Visual range in the polar regions with particular reference to the Alaskan Arctic. *J. Atmos. Terr. Phys.* spec. suppl. 1957-I: 195-211.

Morille, Y., et al., 2007. STRAT: an automated algorithm to retrieve the vertical structure of the atmosphere from single channel lidar data. *J. Atmos. Oceanic Technol.* 24, 761-775.

NASA Earth Observatory. *Natural Hazards*. 8 July 2008. <http://earthobservatory.nasa.gov/NaturalHazards/>

Palm, S., et al., 1996. Remote sensing of the marine atmospheric boundary layer and ocean surface winds: observations from the LITE correlative flights. *1996 International Geoscience and Remote Sensing Symposium, Lincoln, Nebraska*, 1257.

Palm, S., et al., 1998. Inference of marine atmospheric boundary layer moisture and temperature structure using airborne lidar and infrared radiometer data. *J. Appl. Meteor.* 37, 308-324.

Parikh, N.C. and J.A. Parikh, 2002. Systematic tracking of boundary layer aerosols with laser radar. *Optics & Laser Technology* 34: 177-185.

Peixoto, José P. and Abraham H. Oort. *Physics of Climate*. New York: American Institute of Physics, 1992.

Quinn, P. K., et al., 2007. Arctic haze: current trends and knowledge gaps. *Tellus* 59B, 99-114.

Seinfeld, John H. and Spyros N. Pandis. *Atmospheric Chemistry and Physics: from Air Pollution to Climate Change*. 2nd ed. Hoboken, NJ: Wiley, 2006.

Shiobara, M., et al., 2003. A polar cloud analysis based on Micro-pulse Lidar measurements at Ny-Alesund, Svalbard and Syowa, Antarctica. *Physics and Chemistry of the Earth* 28: 1205-1212.

Tjernström, Michael, 2005. The summer Arctic boundary layer during the Arctic Ocean Experiment 2001 (AOE-2001). *Boundary-Layer Meteorology* 177: 5-36.

Wandinger, Ulla. Introduction to Lidar. *Lidar: Range-Resolved Optical Remote Sensing of the Atmosphere*. New York: Springer, 2005.

Warneke, C., et al., 2009. Biomass burning in Siberia and Kazakhstan as an important source for haze over the Alaskan Arctic in April 2008. *Geophys. Res. Lett.* 36, L02813, doi:10.1029/2008GL036194.

Winker, David M., et al., 2007. Initial performance assessment of CALIOP. *Geophys. Res. Lett.* 34, L19803, doi:10.1029/2007GL030135.